

A deep search for 21cm absorption in high redshift damped Lyman- α systems.

Nissim Kanekar^{1*}, Jayaram N Chengalur^{2**}

¹ Kapteyn Institute, University of Groningen, Post Bag 800, 9700 AV Groningen

² National Centre for Radio Astrophysics, Post Bag 3, Ganeshkhind, Pune 411 007

Received mmdyy/ accepted mmdyy

Abstract. We present deep GMRT 21cm absorption spectra of 10 damped Lyman- α systems (DLAs), of which 8 are at redshifts $z \gtrsim 1.3$. HI absorption was detected in only one DLA, the $z = 0.5318$ absorber toward PKS 1629+12. This absorber has been identified with a luminous spiral galaxy; the spin temperature limit ($T_s \leq 310$ K) derived from our observations continues the trend of DLAs associated with bright spirals having low spin temperatures. In seven of the remaining 9 systems, the observations place strong lower limits on the spin temperature of the HI gas.

We combine this sample with data taken from the literature to study the properties of all known DLAs with 21cm absorption studies. The sample of DLAs which have been searched for 21cm absorption now consists of 31 systems, with T_s estimates available in 24 cases; of these, 16 are at $z < 2$ and 8 at $z > 2$, with 11 (all at $z < 1$) having optical identifications. For the latter 11 DLAs, we find that all of the low T_s DLAs have been identified with large, luminous galaxies, while all the DLAs with high spin temperature ($T_s \gtrsim 1000$ K) have been identified either with LSBs or dwarfs. Further, we find no correlation between impact parameter and spin temperature; it is thus unlikely that the high measured T_s values for DLAs arise from lines of sight passing through the outskirts of large disk galaxies. Instead, the spin temperature of DLAs appears to correlate with the host galaxy type.

The trend (noted earlier by Chengalur & Kanekar 2000) that low z DLAs exhibit both high and low T_s values while high redshift ($z \gtrsim 3$) DLAs only show high spin temperatures is present in this expanded data set. Based on this difference in spin temperatures, the Gehan test rules out the hypothesis that DLAs at $z > 2$ and DLAs at $z < 2$ are drawn from the same parent population at $\sim 99\%$ confidence level.

Finally, we use the new GMRT spectra along with 2 spectra from the literature to estimate upper limits on the fraction of cold HI, f_{CNM} , in DLAs at $z \gtrsim 3$. For local spirals, $f_{\text{CNM}} \sim 0.5$; in contrast, we find that $f_{\text{CNM}} < 0.3$ in all 7 high z absorbers, and $f_{\text{CNM}} < 0.1$ in 5 of the 7 cases.

Key words. galaxies: evolution: – galaxies: formation: – galaxies: ISM – cosmology: observations – radio lines: galaxies

1. Introduction

While molecular gas can be detected in emission at high redshifts (albeit only in a handful of somewhat unusual systems), it is as yet a severe challenge to detect neutral atomic gas in emission, even at redshifts as low as $z \sim 0.2$. As a result, absorption spectra against bright background sources provide the sole source of information on neutral atomic gas in the high redshift Universe. An important advantage of using absorption spectra as a probe of systems lying along the lines of sight to distant QSOs is that such studies tend to be unbiased, at least to first order – sources which give rise to absorption are presumably typ-

ical systems at that redshift. In contrast, emission studies of a flux-limited, high redshift sample are usually dominated by the brightest (often atypical) sources.

The large absorption cross-section of the Lyman- α transition and the dominance of hydrogen in baryonic material makes the Lyman- α line one of the easiest to detect in QSO spectra. In fact, lines arising from neutral gas with column densities as low as 10^{13} atoms cm^{-2} can be routinely detected with present day telescopes. However, although these lines (the Lyman- α “forest”) are by far the most numerous, they contain only a small fraction of the total neutral gas at high redshifts; most of the neutral gas is, in fact, contained in relatively rare, high column density ($N_{\text{HI}} \gtrsim 10^{20}$ atoms cm^{-2}) systems, the so-called damped Lyman- α absorbers (DLAs). As the major repository of neutral gas at high redshift, these systems are natural can-

Send offprint requests to: Nissim Kanekar

* nissim@ncra.tifr.res.in

** chengalu@ncra.tifr.res.in

didates for the precursors of today’s galaxies. However, despite their importance in the context of galaxy evolution, the nature of high redshift DLAs is presently quite controversial, with models ranging from large rapidly rotating disks (Wolfe et al. 1986; Prochaska & Wolfe 1997) to merging sub-galactic blobs (Haehnelt et al. 1998) to outflows from dwarf galaxies (Schaye 2001) present in the recent literature.

A successful model for DLAs needs to not only reproduce the observed $\Omega_g(z)$ and column density distribution but also to describe the observed physical conditions in the absorbing gas. The latter is important for our understanding of DLAs, quite independent of their precise size and structure. Conversely, knowledge of these conditions is useful in modelling the further temporal evolution of damped systems. HI 21cm observations (possible only for those DLAs for which the background quasar is also radio loud) are particularly useful because they allow one to estimate the average spin temperature T_s of the absorbing gas. DLA spin temperatures have been, in general, found to be significantly higher than those typically seen in lines of sight through the Galactic disk, or in those through the disks of nearby galaxies (see e.g. Chengalur & Kanekar 2000, Kanekar & Chengalur 2001 and references therein). The only exceptions to the above are DLAs which have been identified as associated with low redshift ($z < 0.6$) spiral galaxies – these systems all have low spin temperatures, comparable to those seen in the Milky Way and nearby spirals. Unfortunately, the number of systems for which deep 21cm observations are available is relatively small; further, while the present data (Chengalur & Kanekar 2000) suggest that high z DLAs are different from low z ones, the observations are currently biased toward systems at $z < 1$, with not too many systems of the sample at high redshift. Are high redshift DLAs indeed systematically different from low redshift ones? Also, how significant is the fact that only DLAs associated with spiral galaxies have low spin temperatures? To find answers to these and similar questions, it is crucial to increase the number of systems with 21cm observations, particularly at high redshifts. We present, in this paper, deep Giant Meterwave Radio Telescope (GMRT) observations of 10 DLAs, 8 of which are at $z > 1$. Two of these systems, the $z = 2.9084$ DLA towards TXS 2342+342 and the $z = 3.0619$ absorber towards PKS 0336–014 have been earlier observed by Carilli et al. (1996); the present observations are far more sensitive than the earlier ones. The observations themselves are summarised in Sect. 2, while the results are presented in Sect. 3 and their implications for physical conditions in DLAs discussed in Sect. 5.

2. Observations and Data Analysis

2.1. The GMRT observations

The GMRT has five currently operational frequency bands, at 150 MHz, 233 MHz, 327 MHz, 610 MHz and 1420 MHz. The present observations utilised the 327,

610 and 1420 MHz bands, which cover redshift ranges $z \sim 2.9 - 3.6$, $z \sim 1.15 - 1.5$ and $z \sim 0 - 0.6$ respectively, with reasonable sensitivity (i.e. better than half the sensitivity at the band centre). The observations were carried out between January and November 2001, using the 30-station FX correlator as the backend; this gives a fixed number of 128 channels over a bandwidth which can be varied between 64 kHz and 16 MHz. All our observations (except for those of PKS 2128–123 (bandwidth = 2 MHz) and PKS 1629+12, which are described below) used a bandwidth of 1 MHz, sub-divided into 128 channels; this gave a channel resolution of 7.8 kHz. The number of available antennas varied between 18 and 26, due to various debugging and maintenance activities. One (or more) of the standard calibrators 3C48, 3C147 or 3C286 was used in all cases to calibrate the absolute flux scale and the system bandpass; these sources were observed at least every two hours in all cases, to ensure a good bandpass calibration. A nearby standard phase calibrator (see Cols. 4 and 5 of Table 1) was observed every forty minutes in all cases to determine the instrumental phase, except in the case of PKS 2128–123 which is itself a phase calibrator for the GMRT. Our experience with the GMRT indicates that the flux calibration is reliable to $\sim 15\%$, in this observing mode. Observational details are summarised in Table 1, where the sources are arranged in order of increasing redshift; note that the values listed here for spectral resolution and RMS noise are before any smoothing.

The only source towards which we detected 21cm absorption, viz. PKS 1629+12, was initially observed with a 1 MHz bandwidth on the 12th and 22nd of October 2001, with 20 antennas and a total on-source time of ~ 6 hours. These observations resulted in the detection of a narrow 21cm absorption feature; the source was hence re-observed on the 17th and 18th of November, 2001 with a 0.25 MHz bandwidth (yielding a resolution of 1.95 kHz, i.e. 0.6 km s^{-1}), to try to resolve out the absorption line. The total on-source time of these latter observations was 13 hours, with 25 antennas. In all cases, 3C286 was used for absolute flux and system bandpass calibration while the compact source 1640+123 was used for phase calibration.

2.2. Data Analysis

The data were analysed in classic AIPS using standard procedures. After the initial flagging and gain and bandpass calibration, continuum images were made for all sources and then used to self-calibrate the U-V data. This was carried out in an iterative manner until the quality of the image was found to not improve on further self-calibration. In general, a few rounds of phase self-calibration were carried out on all fields, followed by one or two rounds of amplitude self-calibration. The continuum emission was then subtracted from the multi-channel U-V data set, using the AIPS task UVSUB; any residual continuum was subtracted by fitting a linear baseline to

Table 1. Observing details

QSO	z_{abs}	ν_{obs} MHz	Phase Cal.	Phase Cal. Flux Jy	No. of antennas	Time Hrs.	Source Flux Jy	Channel resolution km s^{-1}	RMS mJy
PKS 2128–123	0.4298	993.43	^a	^a	20	8	1.90	4.7	1.4
PKS 1629+12	0.5318	927.28	1640+123	2.5	25	13	2.35	0.6	2.8
PKS 0215+015	1.3439	605.72	0204+152	5.0	26	5	0.92	3.9	2.2
QSO 0957+561A	1.3911	594.04	0834+555	7.4	26	6.5	0.59	3.9	2.4
PKS 1354+258	1.4205	586.82	3C286	^b	22	5.5	0.30 ^c	4.0	2.8
TXS 2342+342	2.9084	363.42	3C19	8.3	23	8	0.31	6.4	2.8
PKS 1354–107	2.966	358.15	3C283	21	22	9.5	0.12	6.5	2.0
PKS 0537–286	2.974	357.43	0521–207	7.2	25	5	1.05	6.5	2.4
PKS 0336–014	3.0619	349.69	0323+055	7.4	26	5	0.94	6.7	2.1
PKS 0335–122	3.178	339.97	0409–179	6.1	18	5.5	0.68	6.9	1.9

^a No phase calibrator was used, as PKS 2128–123 is itself a phase calibrator for the GMRT.

^b 3C286 was also used as the flux calibrator; we hence do not have an independent estimate of its flux.

^c PKS 1354+258 is resolved by the GMRT synthesised beam; this is the peak flux.

the U-V visibilities, using the task UVLIN. The continuum subtracted data were then mapped in all channels and a spectrum extracted at the quasar location from the resulting three dimensional data cube. In the case of PKS 1629+12, which showed 21cm absorption, spectra were also extracted from other locations in the cube to ensure that the data were not corrupted by RFI. In general, all the observing frequencies were found to be reasonably free of RFI, except for sporadic interference on individual antennas which was edited out. In the case of multi-epoch observations of a single source, the spectra were shifted to the heliocentric frame outside AIPS and then averaged together.

3. Results

The final absorption spectra towards the ten sources of our sample are shown in Fig. 1, arranged in order of increasing redshift; the measured source fluxes, channel resolutions (in km s^{-1}) and RMS noise values are listed in Cols. 8, 9 and 10 of Table 1.

Our only detection of HI absorption is in the $z = 0.5318$ DLA towards PKS 1629+12. Fig. 2 shows a more detailed version of the GMRT 0.25 MHz HI spectrum towards this source; the spectrum has a resolution of

$\sim 0.6 \text{ km s}^{-1}$ and an RMS noise of 2.8 mJy. Highly asymmetric HI absorption can be clearly seen, extending over a velocity width of $\sim 40 \text{ km s}^{-1}$. The peak absorption occurs at a heliocentric frequency of 927.287 MHz, i.e. at a heliocentric redshift of 0.531787 ± 0.000002 . This lies in between (and in reasonable agreement with) the redshifts of the damped Lyman- α line ($z_{\text{DLA}} = 0.532$; Nestor et al. 2001) and the MgI absorption ($z_{\text{MgI}} = 0.5316$; (Aldcroft et al. 1994; Barthel et al. 1990). (Note that Aldcroft et al. (1994) quote $z = 0.5313$ for the strong MgII and FeII absorption lines.) The flux of PKS 1629+12 was measured to be 2.35 Jy; the peak optical depth is thus $\tau_{\text{max}} = 0.039$. The equivalent width of the profile is $\int \tau dV = 0.494 \pm 0.001 \text{ km s}^{-1}$, obtained by integrating the observed absorption profile.

4. The spin temperature

In the case of an optically thin, homogenous cloud in thermal equilibrium, its HI column density, N_{HI} , 21cm optical depth, τ , and spin temperature, T_s , are related by the expression (e.g. Rohlfs 1986)

$$N_{\text{HI}} = \frac{1.823 \times 10^{18} T_s}{f} \int \tau dV, \quad (1)$$

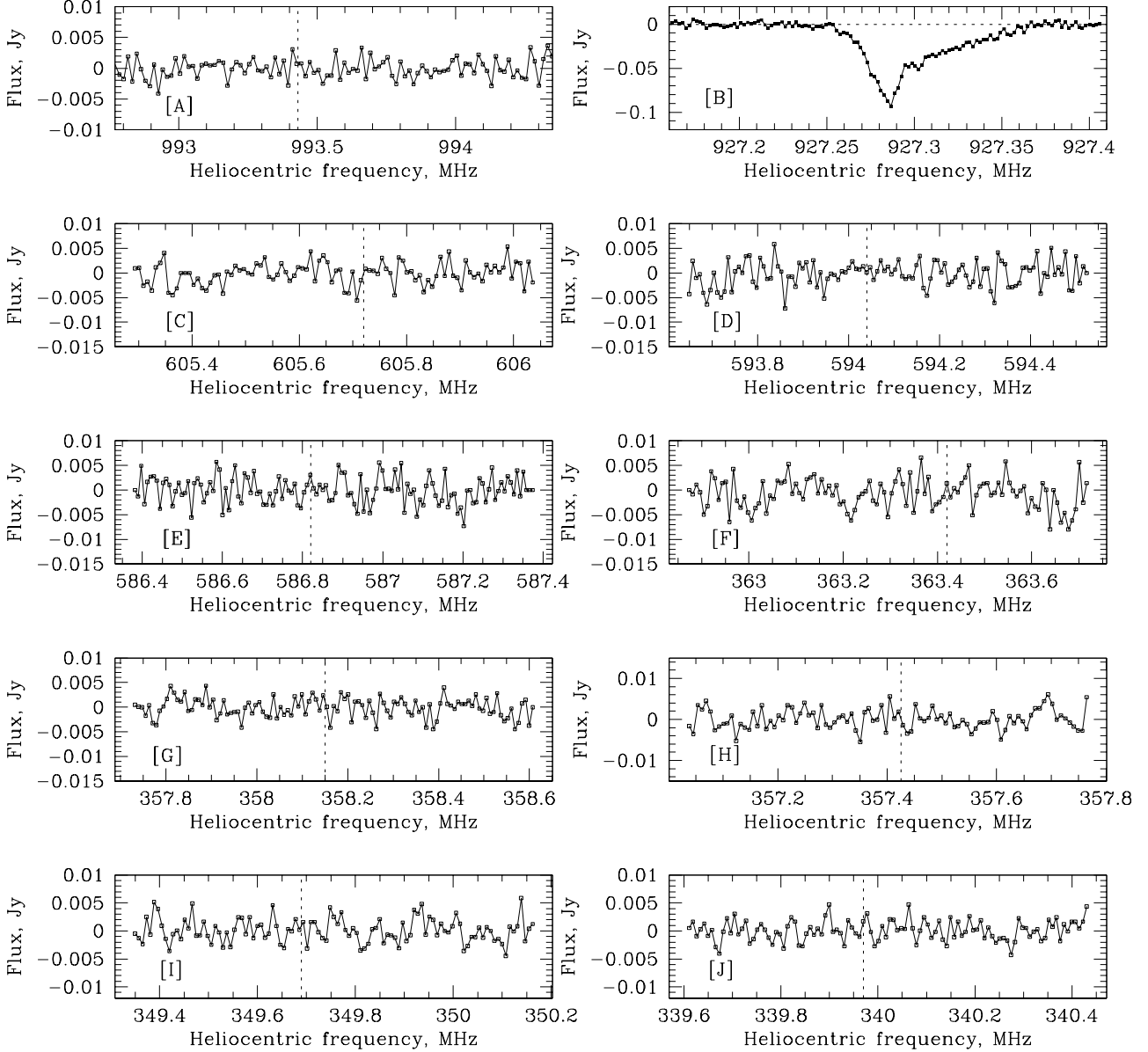


Fig. 1. GMRT HI absorption spectra towards the ten sources of our sample, arranged in order of increasing redshift. [A] $z = 0.4298$ DLA towards PKS 2128–123. [B] $z = 0.5318$ DLA towards PKS 1629+12 [C] $z = 1.3449$ DLA towards PKS 0215+015. [D] $z = 1.3911$ DLA towards QSO 0957+561A. [E] $z = 1.4205$ DLA towards PKS 1354+258. [F] $z = 2.9084$ DLA towards TXS 2342+342. [G] $z = 2.966$ DLA towards PKS 1354–107. [H] $z = 2.974$ DLA towards PKS 0537–286 [I] $z = 3.0619$ DLA towards PKS 0336–014. [J] $z = 3.178$ DLA towards PKS 0335–122.

where N_{HI} is in cm^{-2} , T_s in K and dV in km s^{-1} . f is the covering factor of the absorber. Of course, a given line of sight through an absorber is quite likely to pass through a number of clouds, with different spin temperatures and column densities. In such a situation, the spin temperature obtained using the above expression is the column density weighted harmonic mean of the spin temperatures of the

individual clouds (provided, of course, that all the clouds are optically thin).

It should be noted that Eq. (1) relates the HI column density to the integrated optical depth $\int \tau dV$; this means that, in the case of a non-detection, one needs to know the shape of the absorption profile to compute a lower limit on the spin temperature. This shape is, of

Table 2. The spin temperature for the 10 DLAs observed here

QSO	z_{abs}	$N_{\text{HI}} \times 10^{20}$ cm^{-2}	ΔV ^a km s^{-1}	RMS ^c mJy	τ_{max}^d	$(1/f) \int \tau dV^e$ km s^{-1}	T_s K	Refs. ^f
PKS 2128–123	0.4298	0.25 ± 0.06	7	1.2	< 0.0019	< 0.014	> 980	1
PKS 1629+12	0.5318	2.8	0.6	2.8	0.039	0.494 ± 0.001	310	2
PKS 0215+015	1.3439	0.8	7.8	1.6	< 0.0052	< 0.043	> 1020	3
QSO 0957+561A ^b	1.3911	2.1 ± 0.5	–	–	–	–	–	4
PKS 1354+258 ^b	1.4205	32 ± 2	–	–	–	–	–	4
TXS 2342+342	2.9084	20 ± 0.5	15	2.0	< 0.0192	< 0.306	> 3585	5
PKS 1354–107	2.966	6.0	6.5	2.0	< 0.05	< 0.345	> 955	6
PKS 0537–286	2.974	2.0	10	1.9	< 0.0054	< 0.058	> 1890	6
PKS 0336–014	3.0619	16 ± 1.3	20	1.4	< 0.0045	< 0.095	> 9240	7
PKS 0335–122	3.178	6 ± 1	15	1.2	< 0.0053	< 0.084	> 3920	6

^a ΔV is the FWHM used to compute the spin temperature in the case of non-detections (see the text for more details). For 1629+12, it is the velocity resolution of the observations.

^bThe large uncertainty in the covering factor makes it difficult to estimate the spin temperature (see the text for more details).

^cThis is the RMS actually measured from the smoothed spectra. The spectra were smoothed to a velocity resolution given in the preceding column, except for the following cases for which the RMS was measured at a slightly better spectral resolution than ΔV , viz 12.8 km s^{-1} for TXS 2342+342, 13.4 km s^{-1} for PKS 0336–014 and 13.8 km s^{-1} for PKS 0335–122.

^dAll limits (in this and other columns) correspond to 3σ .

^eThe covering factor f has been set to unity in all cases (see the text for details).

^fReferences for the HI column densities : 1. Ledoux et al. 2002; 2. Nestor et al. 2001; 3. Lanzetta et al. 1995; 4. Rao & Turnshek 2000; 5. White et al. 1993; 6. Ellison et al. 2001a; 7. Prochaska et al. 2001.

course, not a priori known. However, since our limits on the optical depth imply that the HI line is optically thin, the line can be assumed to have a Gaussian shape; here, $\int \tau dV = 1.06\tau_{\text{max}}\Delta V$, where τ_{max} is the peak optical depth (or the limit on the peak) and ΔV is the FWHM of the Gaussian. Further, for a gas cloud in thermal equilibrium, the kinetic temperature T_k (with $T_s \approx T_k$, for a single cloud) and the FWHM of the observed line are related ($T_k \approx 21.855\Delta V^2$, with T_k in K and ΔV in km s^{-1}); care must hence be taken to derive the limits on T_s in a self-consistent manner, so that the velocity width over which the integral is carried out is consistent with (at least) thermal broadening of the gas at the derived temperature (any bulk kinematic motion will further broaden the absorption features; we will assume that no such motions are present). For example, if the 3σ lower limit on the spin temperature is 10000 K, one should use $\Delta V \gtrsim 20 \text{ km s}^{-1}$, while, if the limit is 1000 K, it is appropriate to use $\Delta V \gtrsim 7 \text{ km s}^{-1}$. We have, in the following analysis, used $\Delta V \approx 7, 15$ and 20 km s^{-1} for temperatures $T_s \sim 1000, 5000$ and 10000 K ,

respectively, and have smoothed the spectra to the above resolutions while computing the spin temperature.

The HI column density of a DLA can be directly estimated from the equivalent width of the Lyman- α profile. The original criterion for a system to be classified as a damped absorber ($N_{\text{HI}} \geq 2 \times 10^{20} \text{ cm}^{-2}$) was an observational one, linked to the ability to identify damped profiles in medium resolution spectra from the relatively small telescopes used to carry out the early DLA surveys. Throughout this paper, however, we will consider all systems for which the Lyman- α profile shows damping wings as DLAs, regardless of whether or not their HI column density is greater than the traditionally used threshold. We hence retain the absorbers towards PKS 0215+015 and PKS 2128–123 in our DLA sample, despite their HI column densities being less than 10^{20} cm^{-2} .

Given the HI column density, a search for 21cm absorption directly yields the spin temperature of the absorbing gas (or limits on the temperature, in the case of non-detections of absorption), provided the covering fac-

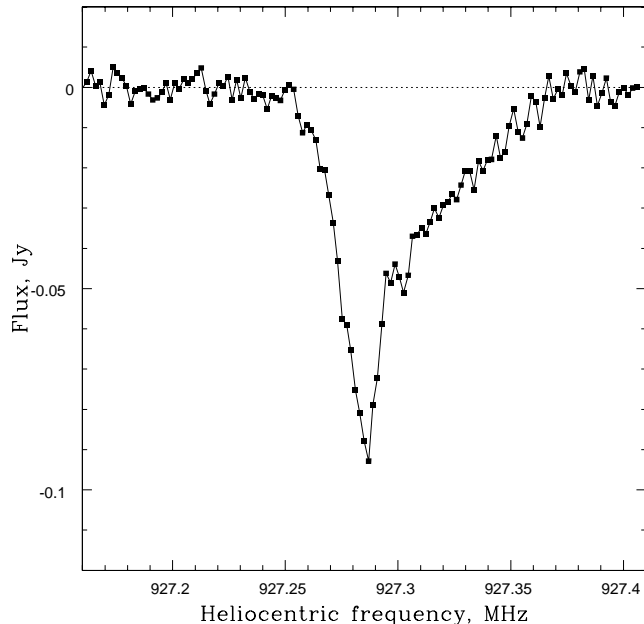


Fig. 2. High resolution (0.6 km s^{-1}) GMRT HI absorption spectrum towards PKS 1629+12. Asymmetric HI absorption is clearly visible, with the peak optical depth at $z = 0.531787$.

tor f is known. Unfortunately, the radio continuum from quasars tends to arise from a far more extended region than the optical or UV emission and it may thus transpire that some fraction of the radio continuum may “leak out” from around the cloud and result in an incorrectly estimated spin temperature. Similarly, the line of sight along which the 21cm optical depth has been measured need not be the same as that for which one has an estimate for the HI column density from the Lyman- α line. The fraction of radio emission originating in compact components spatially coincident with the UV point source can usually, however, be measured from VLBI observations (when such observations are available at sufficiently low frequencies). One can then estimate f and hence, the spin temperature; this is done next, for the ten sources of this paper, in order of increasing right ascension. The results are summarised in Table 2 in which Cols. 4 to 8 contain, respectively, the velocity width ΔV used to compute T_s , the spectral RMS over this (or a slightly smaller) velocity width, the peak optical depth τ_{max} , $(1/f) \int \tau dV$, and the spin temperature T_s (or limits on the last three quantities).

1. VLBA maps of PKS 0215+015 at 2.3 and 8.4 GHz (from the Radio Reference Frame Image Database (RRFID)) show that the source is exceedingly compact, with most of the flux contained within the central 30 milli-arcseconds. The quasar also has a flat spectrum between 8.4 GHz and 610 MHz, again implying that it is quite likely to be compact even at the lower frequencies. It is hence likely that the covering factor f is close to unity. The HI column density of the $z = 1.345$ DLA is $N_{\text{HI}} = 8 \times 10^{19} \text{ cm}^{-2}$ (Lanzetta et al. 1995); the spin tem-

perature of the absorber is then $T_s(3\sigma) > 1020 \text{ K}$ (using $\Delta V = 7.8 \text{ km s}^{-1}$).

2. The $z = 3.178$ DLA towards PKS 0335–122 is the highest redshift system of our sample, with $N_{\text{HI}} = 6 \pm 1 \times 10^{20} \text{ cm}^{-2}$ (Ellison et al. 2001a). Unfortunately, no VLBI information exists in the literature on the background quasar; however, this source has a fairly flat spectrum between 5 GHz and 1.4 GHz, with fluxes of 380 mJy and 420 mJy at these two frequencies. This spectral flatness implies that the flux is likely to arise from a fairly compact source component, which is hence likely to be covered by the DLA. This gives a lower limit to the covering factor, $f \geq 0.7$, which yields $T_s(3\sigma) > 2740 \text{ K}$; if $f = 1$, one has $T_s(3\sigma) > 3920 \text{ K}$ ($\Delta V = 15 \text{ km s}^{-1}$).

3. In the case of PKS 0336–014, 5 GHz VLBI observations (Gurvits et al. 1994) have shown that the source is highly compact at this frequency, with the entire flux contained within the central ~ 7 milli-arcseconds. However, the source also has a negative spectral index, indicating the presence of some extended emission. In the absence of VLBI information at lower frequencies, we will assume a covering factor of unity. The HI column density of the $z = 3.0619$ DLA is $N_{\text{HI}} = 1.6 \pm 0.13 \times 10^{21} \text{ cm}^{-2}$ (Prochaska et al. 2001) giving a spin temperature $T_s(3\sigma) > 9240 \text{ K}$ ($\Delta V = 20 \text{ km s}^{-1}$). Carilli et al. (1996) estimated $T_s > 2500 \text{ K}$ for this DLA.

4. PKS 0537–286 has an exceedingly flat spectrum between 8.4 GHz and 327 MHz; for example, the QSO flux density was measured to be 0.9 Jy at 8 GHz (Parkes survey, Wright & Otrupcek 1990), 1.2 Jy at 4.85 GHz (Griffith et al. 1994), 838 mJy at 1.4 GHz (NRAO-VLA Sky Survey, Condon et al. 1998) and 1.05 Jy in our GMRT 327 MHz image. This implies that the source is likely to be highly compact. VLBA observations at 5 GHz (Fomalont et al. 2000) have shown that the flux within the central 10 milli-arcseconds is ~ 500 mJy, implying a covering factor greater than 0.5. In fact, these observations recovered the entire 5 GHz flux of 1.2 Jy on the shortest VLBA baseline (2×10^6 wavelengths, Hirabayashi et al. 2000), implying that the entire source is contained within ~ 0.1 arcseconds. It is thus quite likely that the covering factor is close to unity; we will use $f = 1$ in this analysis. The HI column density of the $z = 2.9742$ DLA has been found to be $2.0 \times 10^{20} \text{ cm}^{-2}$ (Ellison et al. 2001a); we then obtain a 3σ lower limit of 1890 K on the spin temperature of the absorbing gas ($\Delta V = 10 \text{ km s}^{-1}$).

5. VLBI mapping of QSO 0957+561 has been carried out on a number of occasions, at various frequencies at and above 1.6 GHz (see, for example, Garrett et al. 1994, Campbell et al. 1995). The flux of component A has been measured to be only about 32 mJy at 1.6 GHz (Garrett et al. 1994); clearly, most of the flux seen in the 610 MHz GMRT map comes from extended emission which is unlikely to be covered by the DLA. The covering factor is thus quite uncertain for this absorber, although it is likely to be low. Given this, limits on the spin temperature derived from the present data are unlikely to

be reliable. In fact, it is known that the DLA does not cover the second image (B) of this gravitational lens system (Rao & Turnshek 2000). We will hence not include this system in the later analysis and also do not list limits on the spin temperature and the optical depth in Table 2.

6. PKS 1354+258 is also an extended source at 610 MHz, with no VLBI information available in the literature; the DLA covering factor is hence again quite uncertain. However, the extremely high column density of the absorber ($N_{\text{HI}} = 3.2 \pm 0.2 \times 10^{21} \text{ cm}^{-2}$; Rao & Turnshek 2000) results in high lower limits on the spin temperature even in the case of low covering factors. For example, $f = 0.1$ gives $T_s(3\sigma) > 1100 \text{ K}$, while $f = 1$ would imply $T_s(3\sigma) > 7000 \text{ K}$ (assuming velocity widths of 8 km s^{-1} and 20 km s^{-1} respectively). We will however again not quote a spin temperature in Table 2 due to the uncertainties in the covering factor.

7. No information exists in the literature regarding the VLBI structure of PKS 1354–107. However, the source has a strongly inverted spectrum and is thus likely to be very compact. We will hence assume a covering factor of unity. Combining this with the HI column density of $6 \times 10^{20} \text{ cm}^{-2}$ (Ellison et al. 2001a) gives $T_s(3\sigma) > 955 \text{ K}$ ($\Delta V = 6.5 \text{ km s}^{-1}$).

8. The HI column density of the $z = 0.5318$ DLA towards PKS 1629+12 is $N_{\text{HI}} = 2.8 \times 10^{20} \text{ cm}^{-2}$ (Nestor et al. 2001). PKS 1629+12 is a well-known compact steep spectrum source with an extremely one-sided structure (Saikia et al. 1990). The 2.3 GHz VLBI map of Dallacasa et al. (1998) shows two components with fluxes of 110 mJy and 150 mJy. Only the 110 mJy western component is seen in their 8.4 GHz map, with almost the same flux; they hence identify this as the flat spectrum core of the source. The separation between the two components is 1.14 arcsec (i.e. $\sim 6.4 \text{ kpc}$ at $z = 0.5318$, using $H_0 = 65 \text{ km s}^{-1} \text{ Mpc}^{-1}$ and an $\Omega = 1$, $\Lambda = 0$ cosmology). On the other hand, the core flux density was measured to be 179 mJy at 408 MHz from a $\sim 0.6 \times 0.5$ arcsec resolution Merlin image (Saikia et al. 1990). Using the 2.3 GHz and 408 MHz flux densities to estimate the core spectral index, we obtain a flux density of $\sim 142 \text{ mJy}$ at the redshifted 21cm line frequency of $\sim 927 \text{ MHz}$. If the DLA covers only the core, the spin temperature of the absorber is $T_s \sim 20 \text{ K}$, a remarkably small value. However, the 21cm absorption is spread over $\sim 40 \text{ km s}^{-1}$ and is hence unlikely to arise from a single line of sight. Further, the 408 MHz Merlin map (Saikia et al. 1990) shows that the entire flux at this frequency is contained within ~ 3 arcsecs ($\sim 16.8 \text{ kpc}$ at $z = 0.5318$). It is thus possible that the DLA covers some of the extended flux of the background source, besides the core. VLBI observations in the redshifted 21cm line would be necessary to detect the source components towards which the absorption occurs, and hence, the covering factor. For now, we note that a covering factor of unity results in $T_s = 310 \text{ K}$; this is a definite *upper limit* on the spin temperature, which must then lie between 20 K and 310 K.

9. PKS 2128–123 has a very flat spectrum between 8.4 GHz and 750 MHz, with most measurements between these frequencies yielding a flux density of around 2 Jy (see the NED¹ for details). VLBA maps at 2.3 and 8.4 GHz show that most of this flux is contained within ~ 20 milli-arcseconds, implying that the covering factor is likely to be close to unity. The HI column density of the $z \sim 0.4298$ absorber is $N_{\text{HI}} = 2.5 \pm 0.06 \times 10^{19} \text{ cm}^{-2}$ (Ledoux et al. 2002); the 3σ lower limit on the spin temperature is then $T_s(3\sigma) > 980 \text{ K}$ ($\Delta V = 7 \text{ km s}^{-1}$).

10. Finally, TXS 2342+342 has a fairly flat spectrum between 1.4 GHz and 8 GHz (Wilkinson et al. 1998; White & Becker 1992), indicating that the quasar is very compact at these frequencies. However, as Carilli et al. (1996) point out, the spectrum rises slowly down to the redshifted 21cm frequency of 356 MHz, indicating the presence of a more extended source component. Carilli et al. (1996) argue that the DLA is likely to at least cover the compact component and the covering factor is hence larger than 0.5; it is, however, unclear whether the extended flux is also covered. We will use $f = 1$ in the analysis (following Carilli et al. 1996); the HI column density of $N_{\text{HI}} = 2 \pm 0.5 \times 10^{21} \text{ cm}^{-2}$ then yields $T_s(3\sigma) > 3585 \text{ K}$ ($\Delta V = 15 \text{ km s}^{-1}$). Carilli et al. (1996) estimated $T_s > 1800 \text{ K}$ for this DLA.

5. Discussion

Neutral gas in the galaxy is believed to exist in two stable phases, a cold dense phase (the cold neutral medium, CNM), with typical temperatures of $\sim 100 \text{ K}$, and a warm rarefied phase (the warm neutral medium, WNM), with typical temperatures of $\sim 8000 \text{ K}$. It should be emphasised that such a multi-phase medium exists only over a finite range of interstellar pressures (Wolfire et al. 1995); at higher pressures only the CNM phase exists, while at lower pressures only the WNM phase is found. Further, although the multi-phase structure results from a balance between the heating and cooling rates, which themselves depend on various quantities such as the radiation field, the metallicity, the dust content, etc., it has been shown that a two-phase pressure equilibrium is possible over fairly wide ranges of the above quantities (and, of course, the interstellar pressure; Wolfire et al. 1995). On the observational front, the existence of neutral gas in a multi-phase medium has been established not just for gas in the solar neighborhood, but also in high velocity clouds (e.g. Braun & Burton 2000), dwarf galaxies (e.g. Young & Lo 1997) and DLAs (Lane et al. 2000, Kanekar et al. 2001b). In the latter case of the two DLAs at $z = 0.0912$ and $z = 0.2212$ toward B0738+313, it has been explicitly shown that the observed high spin temperatures are a consequence of 70 – 80 % of the gas being in the warm phase. In this regard, the multi-phase structure of at least these two systems is more like that of dwarf

¹ NASA/IPAC Extragalactic Database

Table 3. Damped Ly- α Systems with 21cm Observations

Name	z_{abs}	N_{HI} 10^{20} cm^{-2}	f	$(1/f) \int \tau dV$ km s^{-1}	ΔV_{21}^a km s^{-1}	T_s^b K	Absorber ID	b^d kpc	Refs.
0738+313 (A)	0.09123	15 ± 2	1	1.0 ± 0.01	40	825 ± 120	Dwarf	< 4	1,2,3
PKS 0439-433 ^c	0.10097	?	1	0.07 ± 0.02	10	?	Spiral ?	8.0	4,5
0738+313 (B)	0.22125	7.9 ± 1.4	1	0.488 ± 0.004	30	890 ± 165	Dwarf	20	1,3,6
PKS 0952+179	0.23779	21 ± 2.5	0.25	0.56 ± 0.02	30	2055 ± 330	LSB	< 7	7,8,9
PKS 1413+135 ^{c*}	0.24671	200*	0.12	59.43	39	185	Spiral	?	10,11,12
PKS 1127-145	0.3127	51 ± 9	1	3.074 ± 0.002	120	910 ± 160	LSB	< 10	8,9,13
PKS 1229-021	0.39498	5.6 ± 0.5	0.5	1.81 ± 0.01	110	170 ± 15	Spiral	11	14,15,16
QSO 0248+430	0.3941	?	?	2.99	40	?	-	-	17
PKS 2128-123	0.4298	0.25 ± 0.06	1	< 0.014	-	> 980	-	-	18,19
3C196	0.43670	6.3 ± 1.6	?	?	250	-	Spiral	9.2	14,20,21
PKS 1243-072	0.4367	?	1	0.38	23	?	Spiral	11.3	17,22
3C446 ^c	0.4842	6.3	0.1	< 0.22	-	> 1570	-	-	13,23
A0 0235+164	0.524	50	1	13 ± 0.6	125	210	Spiral	< 11.2	24,25,26
B2 0827+243	0.5247	2.0 ± 0.2	0.67	0.33 ± 0.03	50	330 ± 70	Spiral	34	7,8,9
PKS 1629+12	0.5318	2.8	1	0.494 ± 0.001	40	310	Spiral	17	9,19
PKS 0118-272 ^c	0.5579	?	0.5	< 0.12	-	?	-	-	7,27
3C286	0.69215	20 ± 1.6	1 ?	0.91 ± 0.09	18	1205 ± 240	LSB	19	15,28,29
PKS 0454+039	0.8596	5 ± 0.16	1	< 0.32	-	> 855	Dwarf	6.4	15,30,31
PKS 0215+015 ^c	1.3449	0.8	1	< 0.043	-	> 1020	-	-	19,32
QSO 0957+561A	1.3911	2.1 ± 0.5	?	-	-	-	-	-	8,19
PKS 1354+258	1.4205	32 ± 2	-	-	-	-	-	-	8,19
MC3 1331+170	1.77636	15 ± 1.5	0.8	0.5 ± 0.1	25	1645 ± 615	-	-	31,33,34
PKS 1157+014	1.944	63 ± 10	0.55	4 ± 0.2	60	865 ± 190	-	-	31,35,36
PKS 0458-02	2.03945	45 ± 8	1	6.4 ± 0.4	30	385 ± 100	-	-	34,37,47
PKS 0528-2505	2.8110	22 ± 1	1	< 1.70	-	> 710	-	-	38,39,40
TXS 2342+342	2.9084	20 ± 0.5	1	< 0.306	-	> 3585	-	-	19,41
PKS 1354-107	2.966	6	1	< 0.345	-	> 955	-	-	19,42
PKS 0537-286	2.9742	2	1	< 0.058	-	> 1890	-	-	19,42
PKS 0336-014	3.0619	16 ± 1.3	1	< 0.095	-	> 9240	-	-	19,41,46
PKS 0335-122	3.178	6 ± 1	1	< 0.084	-	> 3920	-	-	19,42
PKS 0201+113	3.3875	18 ± 3	1	< 0.30	-	> 3290	-	-	41,44,45

* The $z = 0.24671$ absorber towards PKS 1413+135 may be an ‘‘associated’’ absorption system, rather than an intervening one (Perlman et al. 2002). Further, its HI column density is estimated from an X-ray spectrum (Stocke et al. 1992).

^a The velocity width ΔV quoted here is the entire velocity range over which absorption is seen.

^b The spin temperature values (or 3σ limits) quoted here have been consistently (re-)computed from the published data using Eq. (1), and the latest available values for all parameters in the equation. The values quoted here and the errors have been rounded off to the nearest 5 K. The errors on N_{HI} and hence, on T_s , have been quoted when available in the original references; in the case of asymmetric errors, the larger value has been quoted. In certain instances, the values may differ slightly from that quoted by the authors in the original reference. The only exception is PKS 0201+113, for which multiple and quite different values are quoted in the literature. We use the value from Kanekar & Chengalur (1997), modified by the new HI column density of $1.8 \pm 0.3 \times 10^{21} \text{ cm}^{-2}$, from Ellison et al. (2001b).

^c Candidate damped Lyman- α systems, based on IUE spectra, metal lines or X-ray spectra.

^d The impact parameter b has been calculated using an $\Omega = 1$, $\Lambda = 0$ Universe, with $H_0 = 65 \text{ km s}^{-1} \text{ Mpc}^{-1}$.

¹ Rao & Turnshek 1998, ² Chengalur & Kanekar 1999, ³ Cohen 2001, ⁴ Petitjean et al. 1996, ⁵ Kanekar et al. 2001a, ⁶ Kanekar et al. 2001b, ⁷ Kanekar & Chengalur 2001, ⁸ Rao & Turnshek 2000, ⁹ Nestor et al. 2001, ¹⁰ Stocke et al. 1992, ¹¹ Carilli et al. 1992, ¹² Perlman et al. 2002. ¹³ Chengalur & Kanekar 2000, ¹⁴ Kanekar & Chengalur 2002, ¹⁵ Boisse et al. 1998, ¹⁶ le Brun et al. 1997, ¹⁷ Lane & Briggs 2002, ¹⁸ Ledoux et al. 2002, ¹⁹ This paper, ²⁰ Briggs et al. 2001, ²¹ Cohen et al. 1996, ²² Kanekar et al. 2002, ²³ Lanzetta et al. 1995, ²⁴ Roberts et al. 1976, ²⁵ Burbidge et al. 1996, ²⁶ Cohen et al. 1999, ²⁷ Vladilo et al. 1997, ²⁸ Steidel et al. 1994, ²⁹ Davis & May 1978, ³⁰ Steidel et al. 1995, ³¹ Briggs et al. 1983, ³² Turnshek & Rao 2002, ³³ Wolfe & Davis 1979, ³⁴ Pettini et al. 1994, ³⁵ Briggs et al. 1984, ³⁶ Wolfe et al. 1981, ³⁷ Wolfe et al. 1985, ³⁸ Carilli et al. 1996, ³⁹ Morton et al. 1980, ⁴⁰ Foltz et al. 1988, ⁴¹ White et al. 1993, ⁴² Ellison et al. 2001a, ⁴³ Ellison et al. 2001b, ⁴⁴ Kanekar & Chengalur 1997, ⁴⁵ Briggs et al. 1997, ⁴⁶ Prochaska et al. 2001, ⁴⁷ Prochaska & Wolfe 1999.

galaxies (see, for example, Young & Lo 1997) than large spiral disks.

Table 3 contains a list of the 31 known candidate and confirmed DLAs for which 21cm observations are available in the published literature (this is an update of the list in Chengalur & Kanekar 2000). Note that the Lyman- α line has so far not been observed for the DLAs at $z = 0.24671$ towards PKS 1413+135, $z = 0.3941$ towards QSO 0248+430 and $z = 0.43669$ towards PKS 1243-072; however, all three systems show strong 21cm absorption, implying (for reasonable values of T_s) HI column densities higher than 10^{20} cm^{-2} (Carilli et al. 1992; Kanekar et al. 2002; Lane & Briggs 2002) and have hence been included in the present sample. Further, the $z = 0.24671$ absorber towards PKS 1413+135 may be an associated system (Perlman et al. 2002); the HI column density listed in Table 3 is estimated from the deficit of soft X-rays (Stocke et al. 1992). No similar direct estimate exists for the HI column densities of the systems towards PKS 1243-072 and QSO 0248+430. We also note that two candidate DLAs (on the basis of metal lines), at $z = 0.5579$ towards PKS 0118-272 (Kanekar & Chengalur 2001) and $z = 0.101$ towards PKS 0439-433 (Kanekar et al. 2001a) have, for completeness, been included in this table; however, they will not be used in the later analysis, as their HI column densities (and hence, spin temperatures) are unknown. Cols. 3, 4, 5, 6 and 7 of the table contain the HI column density (in units of 10^{20} cm^{-2}), the adopted covering factor f , the “true” equivalent width ($(1/f) \int \tau dV$), the velocity spread of 21cm absorption (between nulls, in km s^{-1}) and the spin temperature. Besides these, Cols. 8 and 9 list the nature of the objects identified as the DLA hosts and their impact parameters (b , in kpc) to the QSO line of sight. Of course, it is possible that the latter identifications are in error in some cases if, for example, the absorption arises in an object closer to the QSO but too faint to be identified in optical/IR images. With this caveat in mind, we note that seven of the DLA hosts have been identified with large, luminous galaxies, with luminosities close to L_* .

Fig. 3 shows a plot of the measured spin temperatures as a function of redshift for the 24 DLAs of the complete sample which have reliable estimates of the spin temperature (note that this plot includes the $z = 0.24671$ absorber towards PKS 1413+135 which may be an associated system). The seven systems in Table 3 which are not included in Fig. 3 are the two 21cm absorbers towards PKS 1243-072 and QSO 0248+430 for which the HI column density is unknown (see above), the DLAs towards PKS 1354+258 and QSO 0957+561 for which the covering factor is highly uncertain (see Sect. 4), the two candidate DLAs towards PKS 0118-272 and PKS 0439-433 and, finally, the $z = 0.437$ absorber towards 3C196, where the lines of sight to the optical QSO and the radio continuum trace very different paths through the absorbing galaxy. The dotted line in Fig. 3 is at 350 K – more than 80 % of spin temperature measurements in M 31 and the Milky Way have values < 350 K (Braun & Waltherbos 1992). It

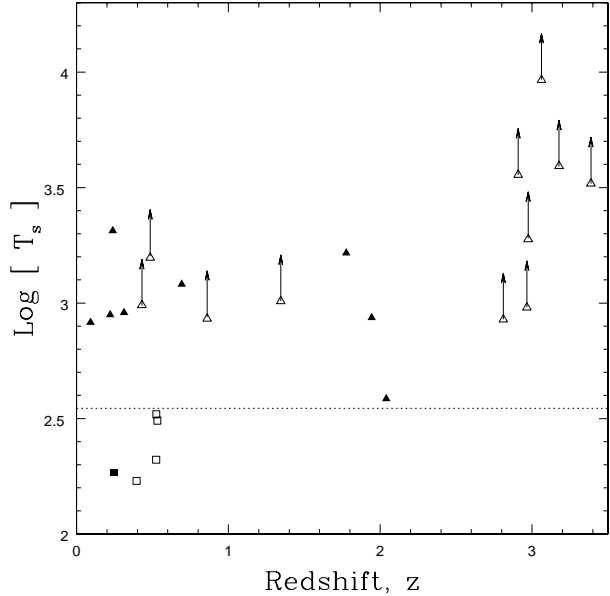


Fig. 3. The spin temperature ($\text{Log}[T_s]$) of the 24 DLAs of the complete sample with T_s estimates as a function of redshift z . Note that seven DLAs listed in Table 3 have not been included here for reasons listed in the text. Objects identified with spiral galaxies are plotted using squares; the filled square shows the $z = 0.24671$ spiral towards PKS 1413+135, which may be an associated system. Other detections are shown as filled triangles, with non-detections shown as open triangles, with arrows.

can be seen that the spin temperatures of the majority of DLAs are considerably higher than those typical of lines of sight through the disks of the Milky Way or nearby spiral galaxies. The only exceptions to the above are the five systems at low z which have been identified with spiral disks and the DLA at $z \sim 2.04$ towards PKS 0458-020, for which $T_s \sim 385 \pm 100$ K; we discuss the latter separately below. Note that it is not presently possible to estimate the spin temperatures of the remaining two $L \sim L_*$ DLAs at $z \sim 0.437$ towards PKS 1243-072 and 3C196. Finally, the 21cm absorption profile for PKS 1629+12 reported in this paper continues the trend (noted earlier in Chengalur & Kanekar (2000) and Kanekar & Chengalur (2001)) of low spin temperatures being found in all DLAs identified as $L \sim L_*$ galaxies.

Fig. 4 presents the data in an alternative way, as a scatter plot of the “true” HI 21cm equivalent width (i.e. $(1/f) \int \tau dV$) against the HI column density. Both of these are directly observable quantities. The crosses show the same quantities for Galactic HI clouds (Colgan et al. 1988; Payne et al. 1982), measured using 21cm absorption/emission studies. HI column density estimates using observations of the Lyman- α line have been found to be in good agreement with estimates from 21cm emission studies (Dickey & Lockman 1990). Fig. 4 hence allows a direct comparison of the same observables for DLAs and galactic clouds. It can be clearly seen that, at

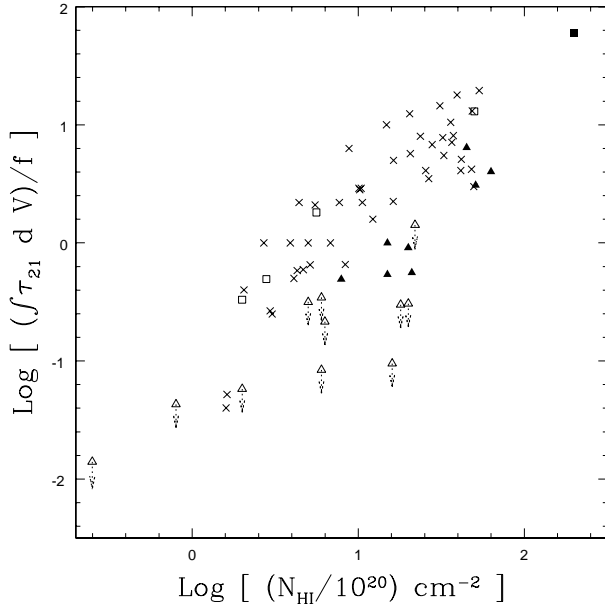


Fig. 4. The *true* equivalent width ($\int \tau dV/f$) as a function of the HI column density for the 24 DLAs of the complete sample for which we can calculate T_s values. Objects identified with spiral galaxies are plotted using squares; the filled square shows the $z = 0.24671$ spiral towards PKS 1413+135, which may be an associated system. Other detections are shown as filled triangles, with non-detections shown as open triangles, with arrows. The crosses show measurements in the Galaxy by Colgan et al. (1988) and Payne et al. (1982), using 21cm emission/absorption studies.

a given HI column density, the majority of DLAs tend to have smaller 21cm equivalent widths than those found for lines of sight through the Galaxy. The only exceptions are DLAs that are known to be associated with spiral galaxies (shown as squares) and the $z \sim 2.04$ DLA towards PKS 0458–020, (which we discuss in more detail below), which do lie within the range of Galactic values. The conclusion would seem to be that the majority of DLAs contain larger fractions of the warm (and thus weakly absorbing) phase of neutral hydrogen than typical in nearby spirals, as earlier pointed out by Carilli et al. (1996) and Kanekar & Chengalur (2001).

It is possible that the high T_s values seen in DLAs might arise due to absorption originating in the outskirts of large disks, which would also provide a higher absorption cross-section than the inner regions of these galaxies. Fig. 5 shows a plot of T_s versus impact parameter b for the 10 DLAs of the sample (all with $z < 1$) with optical identifications, as well as estimates of both T_s and impact parameter; absorbers identified with spiral galaxies are shown as open squares. No correlation can be seen to exist between T_s and b . On the contrary, the largest impact parameter of the sample ($b = 34$ kpc) is seen in a low T_s system, the $z = 0.5247$ DLA towards B2 0827+243, while four of the high T_s DLAs have $b < 10$ kpc. The low

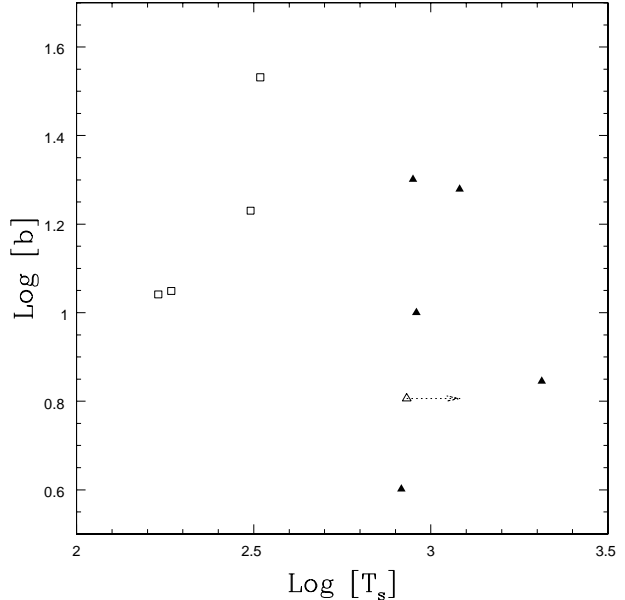


Fig. 5. The impact parameter b (in kpc) as a function of spin temperature for 10 DLAs at $z < 1$. The open squares represent objects identified with spiral galaxies; the remaining detections are shown as filled triangles, with non-detections shown as open triangles, with arrows.

redshift sample clearly does not support the hypothesis that the high T_s seen in low redshift DLAs is because the absorption arises from lines of sight which pass through the outer regions of disk galaxies. Instead, it appears that the spin temperature correlates with the nature of the absorbing galaxy. We discuss next the $z \sim 2.04$ DLA towards PKS 0458–020, the only high z DLA with a spin temperature $T_s < 400$ K.

The $z = 2.03945$ DLA towards PKS 0458–020 is as yet the highest redshift DLA with a confirmed detection of 21cm absorption (Wolfe et al. 1985). Briggs et al. (1989) found the VLBI 21cm absorption profile to be very similar to the single dish profile and used this to argue that the absorber shows little structure on the scale of the extended radio continuum emission of the background source; these observations hence imply that the transverse size of the absorber is larger than $8 h^{-1}$ kpc. Further, the low ionization metal lines of the DLA are clearly asymmetric (Prochaska & Wolfe 1997), which can be explained if the absorber is a rapidly rotating disk (although such asymmetries are also explainable in other models; see, for example, Haehnelt et al. 1998, McDonald & Miralda-Escude 1999). The spin temperature of the absorber was originally estimated to be $T_s = 594 \pm 297$ K (Wolfe et al. 1985), the large error arising due to uncertainties in fitting the Lyman- α profile ($N_{\text{HI}} = 8 \pm 4 \times 10^{21} \text{ cm}^{-2}$; Wolfe et al. 1985). Recently, however, the HI column density has been measured far more accurately by Pettini et al. (1994), who quote $N_{\text{HI}} = 4.5 \pm 0.8 \times 10^{21} \text{ cm}^{-2}$. Combining this with the HI 21cm absorption profile (and taking $f = 1$, as confirmed by the

Table 4. The CNM fraction in high z DLAs.

Name	z_{abs}	N_{HI} (200 K) $\times 10^{20}$	N_{HI} (Total) $\times 10^{20}$	f_{CNM}
PKS 0528–250	2.8110	<6.2	22 ± 1	<0.28
TXS 2342+342	2.9084	<0.7	20 ± 0.5	<0.03
PKS 1354–107	2.966	<1.3	6.0	<0.21
PKS 0537–286	2.9742	<0.2	2.0	<0.09
PKS 0336–014	3.0619	<0.2	16 ± 1.3	<0.01
PKS 0335–122	3.178	<0.2	6 ± 1	<0.04
PKS 0201+113	3.3875	<1.1	18 ± 3	<0.06

VLBI observations) yields $T_s = 385 \pm 100$ K, a value not too far from those obtained in local spirals; this is the first case of a DLA at $z \gtrsim 0.6$ with a spin temperature less than 400 K. Interestingly enough, the 21cm equivalent width of the absorber too lies close to the range of Galactic values shown in Fig. 4. We note, however, that the metallicity of the absorber is far lower than solar values ($[Zn/H] = -1.16 \pm 0.09$; Prochaska & Wolfe 1999), implying that the DLA has not undergone much chemical evolution. Detailed analysis of the formation of a multi-phase medium in proto-galaxies (Spaans & Carollo 1997; Spaans & Norman 1997) indicate that the epoch of formation of a multi-phase ISM is a strong function of the galactic mass; galaxies with baryonic mass $\sim 5 \times 10^{11} M_\odot$ form the cold phase by $z \sim 3$ while dwarf galaxies, with baryonic mass $\sim 3 \times 10^9 M_\odot$, typically form the cold phase only by $z \sim 1$. The relatively low measured spin temperature in the $z \sim 2.04$ DLA thus makes it likely that the absorber is a large galaxy. The VLBI observations and the low spin temperature are hence both consistent with the DLA being a massive galaxy, with the high mass providing a sufficiently high central pressure to compensate for the low metallicity and produce a sizeable fraction of the cold phase of HI.

The evolution of spin temperature with redshift has been the subject of interest for some time. The original observations of high spin temperatures at high redshift led to the suggestion that the elevation of the spin temperature was perhaps due to evolutionary effects. More recently, the detection of low redshift DLAs ($z \lesssim 0.2$) with high T_s values (Lane et al. 1998, Chengalur & Kanekar 1999) indicated that a simple trend did not exist in the evolution of T_s with redshift. However, Chengalur & Kanekar (2000) noted the following trend: DLAs with both low and high spin temperatures are found at low redshifts ($z \lesssim 1$), while only high T_s DLAs are found at high redshifts ($z \gtrsim 3$). The present, larger sample of Fig. 3 shows this trend clearly, with the exceedingly high values of spin temperature at $z \gtrsim 3$ indicating that these systems contain very small fractions of the CNM phase of HI.

The non-detection of HI absorption in the present fairly deep search can be used to place stringent constraints on the fractional content of CNM in the high z absorbers. To do so, we note that the allowed values of CNM temperatures in the Milky Way lie between 40 K and 200 K (Wolfire et al. 1995). We hence use 200 K (in Eq. (1)) as an upper limit to the temperature of the CNM phase in the seven $z \gtrsim 3$ DLAs to estimate upper limits on the CNM fraction in these systems. The original high resolution spectra (see Table 1) are used for this purpose, not the smoothed spectra used to estimate the spin temperature. The results are shown in Table 4 where the third column gives the 3σ upper limit to the HI column density in 200 K gas (note that this limit scales linearly with the assumed CNM temperature and would hence be even lower for lower temperature CNM). The last column in this table gives the upper limit to the fraction of the HI in CNM, f_{CNM} ; it can be seen that five of the seven systems at $z \gtrsim 3$ have CNM fractions less than 10 %, with three of these having $f_{\text{CNM}} < 5$ %. Clearly, most of the gas in the high z DLAs is warm, the typical fraction of CNM gas is even smaller than that in the two high T_s DLAs at low redshift with measured CNM fractions (Lane et al. 2000, Kanekar et al. 2001b) or in local dwarf galaxies (Young & Lo 1997).

An independent line of evidence for high temperatures at high redshift comes from observations of the $n(\text{CII})/n(\text{CI})$ ratio (Liszt 2002), which is quite different in the CNM and the WNM. Liszt (2002) used observations of this ratio in 11 DLAs to suggest that high redshift ($z > 2.3$) DLAs are dominated by warm gas, with at most a few per cent of the neutral HI in the CNM. This is in agreement with our results. Besides this, it has been observed that high z DLAs typically have very low molecular gas fractions; this can be understood in models in which the absorbing gas is at high temperature (Petitjean et al. 2000; but see also Liszt 2002). We note, in passing, that it is exceedingly interesting that the $z = 3.0619$ DLA towards PKS 0336–014 has $T_s > 9240$ K, implying that its gas is significantly hotter than even the standard WNM in the Milky Way (which has temperatures in the range 5000 – 8000 K; Wolfire et al. 1995).

Of the 24 DLAs with T_s measurements, 16 are at $z < 2$ and 8 at $z > 2$; we will call these the low and high z samples respectively. The sample is of a sufficiently large size to carry out a statistical comparison to test the likelihood that the systems in the two samples stem from the same parent distribution. The Gehan test (Gehan 1965; Miller 1981) is appropriate for this comparison as it can be directly used in the case of limits on the measured quantity (in our case, the spin temperature). When applied to our data, this test rules out the possibility of the two samples being drawn from the same distribution at the $\sim 99\%$ confidence level. (If one chooses to treat the 3σ upper limits as detections, a Kolmogorov-Smirnov rank 1 test rules out the above hypothesis at the 95 % confidence level.) It is thus very unlikely that the high and low z DLAs are systems of similar “character”. We note

that $z = 2$ was used as the redshift of separation of the two samples as this is the approximate redshift where star formation is believed to peak; it is hence plausible that systems at $z > 2$ will show differences from those at lower redshifts. Since we have only 4 systems with T_s estimates in the redshift range $1 < z < 2.8$ (the $z \sim 1.4$ DLAs towards PKS 1354+258 and QSO 0957+561A do not have good estimates of T_s), it is not possible to independently determine the threshold redshift with the present sample.

In conclusion, the sample of damped Lyman- α systems which have been searched for 21cm absorption now consists of 31 systems; estimates of the spin temperature are available in 24 cases, of which 16 DLAs are at $z < 2$ and 8 at $z > 2$. All of the low T_s , low z DLAs have been identified with large, luminous galaxies, while all DLAs at $z < 1$ with high spin temperature ($T_s \gtrsim 1000$ K) have been identified either with LSBs or dwarfs. It thus appears likely that the spin temperature depends mainly on the nature of the absorbing galaxy, as suggested earlier by Chengalur & Kanekar (2000). We use a recent measurement of the HI column density in the $z = 2.03945$ DLA towards PKS 0458–020 to derive a relatively low T_s value in the absorber; this is the first high z DLA to show $T_s < 400$ K. The low metallicity allied with a low spin temperature suggest that the DLA is a massive galaxy, consistent with VLBI limits of its transverse size. The new deep GMRT 21cm spectra of this paper have also been used to estimate the fraction of HI in the cold phase, f_{CNM} , in the absorbers at $z \gtrsim 3$; it was found that $f_{\text{CNM}} < 0.3$ in all seven absorbers, with $f_{\text{CNM}} < 0.1$ in five of the seven cases. These results are in good agreement with estimates of $f_{\text{CNM}} \sim \text{few } \%$, from observations of the $n(\text{CII})/n(\text{CI})$ ratio (Liszt 2002). Finally, we have used the above spin temperature estimates to test the likelihood that the $z > 2$ and $z < 2$ DLAs are drawn from the same parent population and rule out this hypothesis at the $\sim 99\%$ confidence level.

Acknowledgements. We thank the referee, Wendy Lane, for numerous suggestions and comments on an earlier version which have significantly improved this paper. These observations would not have been possible without the many years of dedicated effort put in by the GMRT staff in order to build the telescope. The GMRT is operated by the National Centre for Radio Astrophysics of the Tata Institute of Fundamental Research. This research has made use of the United States Naval Observatory (USNO) Radio Reference Frame Image Database (RRFID) and the NASA/IPAC Extragalactic Database (NED) which is operated by the Jet Propulsion Laboratory, California Institute of Technology, under Contract with the National Aeronautics and Space Administration.

References

- Aldcroft T. L., Bechtold J. & Elvis M., 1994, ApJS 93, 1
 Barthel P. D., Tytler D. R. & Thomson B., 1990, A&AS 82, 339
 Boissé P., le Brun V., Bergeron J. & Deharveng J.-M., 1998, A&A 333, 841
 Braun R. & Walterbos R. A. M., 1992, ApJ 386, 120.
 Braun R. & Burton W. B., 2000, A&A 354, 853.
 Briggs F. H. & Wolfe A. M., 1983, ApJ 268, 76
 Briggs F. H., Turnshek D. A. & Wolfe A. M., 1984, ApJ 287, 549
 Briggs F. H., Wolfe A. M., Liszt H. S., Davis M. M. & Turner K. L., 1989, ApJ 341, 650
 Briggs F. H., Brinks E. & Wolfe A. M., 1997, AJ 113, 467
 Briggs F. H., de Bruyn A. G. & Vermeulen R. C., 2001, A&A 373, 113
 le Brun V., Bergeron J., Boissé P. & Deharveng J.-M., 1997, A&A 321, 733
 Burbidge E. M., Beaver E. A., Cohen R. D., Junkkarinen V. T. & Lyons R. W., 1996, AJ 112, 2533
 Campbell R. M., Lehar J., Corey B. E., Shapiro I. I. & Falco E. E., 1995, AJ 110, 2566
 Carilli C. L., Perlman E. S. & Stocke J. T., 1992, ApJ 400, L13
 Carilli C. L., Lane W., de Bruyn A. G., Braun R. & Miley G. K., 1996, AJ 111, 1830
 Cohen R. D., Beaver E. A., Diplas A. et al., 1996, ApJ 456, 132
 Cohen R. D., Burbidge E. M., Junkkarinen V. T., Lyons R. W. & Madejski G., 1999, BAAS 194.7101
 Cohen J. G., 2001, AJ 121, 2895
 Colgan S. W. J., Salpeter E. E. & Terzian Y., 1988, ApJ 328, 275
 Condon J. J., Cotton W. D., Greisen E. W. et al., 1998, AJ 115, 1693
 Chengalur J. N. & Kanekar N., 1999, MNRAS 302, L29
 Chengalur J. N. & Kanekar N., 2000, MNRAS 318, 303
 Dallacasa D., Bondi M., Alef W. & Mantovani F., 1998, A&AS 129, 219
 Davis M. M. & May L. S., 1978, ApJ 219, 1
 Dickey J. & Lockman F. J., 1990, ARA&A 28, 215
 Ellison S. L., Yan L., Hook I. M. et al., 2001a, A&A 379, 393
 Ellison S. L., Pettini M., Steidel C. C. & Shapley A. E., 2001b, ApJ 549, 770
 Foltz C. B., Chaffee Jr. F. H. & Black J. H., 1988, ApJ 324, 267
 Fomalont E. B., 2000, ApJS 131, 95
 Garrett M. A., Calder R. J., Porcas R. W. et al., 1994, MNRAS 270, 457
 Gehan E. A., 1965, Biometrika 52, 203
 Griffith M. R., Wright A. E., Burke B. F. & Ekers R. D., 1994, ApJS 90, 179
 Gurvits L. I., Schilizzi R. T., Barthel P. D. et al., 1994, A&A 291, 737
 Haehnelt M. G., Steinmetz M. & Rauch M., 1998, ApJ 495, 64
 Hirabayashi H., Fomalont E. B., Horiuchi S. et al., 2000, PASJ 52, 997
 Kanekar N. & Chengalur J. N., 1997, MNRAS 292, 831
 Kanekar N., Chengalur J. N., Subrahmanyam R. & Petitjean P., 2001a, A&A 367, 46
 Kanekar N., Ghosh T. & Chengalur J. N., 2001b, A&A 373, 394
 Kanekar N. & Chengalur J. N., 2001, A&A 369, 42
 Kanekar N., Athreya R. & Chengalur J. N., 2002, A&A 382, 838
 Kanekar N. & Chengalur J. N., 2002, in preparation
 Lane W., Smette A., Briggs F. H. et al., 1998, AJ 116, 26.
 Lane W., Briggs F. H. & Smette A., 2000, ApJ 532, 146
 Lane W. & Briggs F. H., 2002, ApJ 561, L27
 Lanzetta K. M., Wolfe A. M. & Turnshek D. A., 1995, ApJ 440, 435

- Ledoux C., Bergeron J. & Petitjean P., 2002, *A&A* 385, 802
- Liszt H., 2002, *A&A* 389, 393
- McDonald P. & Miralda-Escude J., 1999, *ApJ* 519, 486
- Miller Jr., R. G., 1981, *Survival Analysis* (John Wiley & Sons)
- Morton D. C., Jian-sheng C., Wright A. E., Peterson B. A. & Jauncey D. L., 1980, *MNRAS* 193, 399
- Nestor D. B., Rao S. M., Turnshek D. A. et al., 2001, in “Extragalactic Gas at Low Redshift”, J. S. Mulchaey & J. T. Stocke (eds.), *ASP Conference Series* 254, 34
- Payne H. E., Salpeter E. E. & Terzian Y., 1982, *ApJS* 48, 199
- Perlman E. S., Stocke J. T., Carilli C. L. et al., 2002, *AJ*, 124, 2401
- Petitjean P., Théodore B., Smette A. & Lespine Y., 1996, *A&A* 313, L25
- Petitjean P., Srianand R. & Ledoux C., 2000, *A&A* 364, L26
- Pettini M., Smith L. J., Hunstead R. W. & King D. L., 1994, *ApJ* 426, 79
- Pettini M., King D. L., Smith L. J. & Hunstead R. W., 1997, *ApJ* 478, 536
- Prochaska J. X. & Wolfe A. M., 1997, *ApJ* 487, 73
- Prochaska J. X. & Wolfe A. M., 1999, *ApJS* 121, 369
- Prochaska J. X., Wolfe A. M., Tytler D. et al., 2001, *ApJS* 137, 21
- Rao S. M. & Turnshek D. A., 1998, *ApJ* 500, L115
- Rao S. M. & Turnshek D. A., 2000, *ApJS* 130, 1
- Roberts M. S., Brown R. L., Brundage W. D. et al., 1976, *AJ* 81, 293.
- Rohlfs K., 1986, *Tools of Radio Astronomy* (Springer-Verlag, Berlin Heidelberg)
- Saikia D. J., Junor W., Cornwell T. J., Muxlow T. W. B. & Shastri P., 1990, *MNRAS* 245, 408
- Schaye J., *ApJ* 559, L1
- Spaans M. & Carollo C. M., 1997, *ApJ* 482, L3
- Spaans M. & Norman C. A., 1997, *ApJ* 483, 87
- Steidel C. C., Pettini M., Dickinson M. & Persson S. E., 1994, *ApJ* 437, 75
- Steidel C. C., Bowen D. V., Blades J. C. & Dickson M., 1995, *ApJ* 440, L45
- Stocke J. T., Wurtz R., Wang Q., Elston R. & Jannuzi B. T., 1992, *ApJ* 400, L17
- Turnshek D. A. & Rao S. M., 2002, *ApJ* 572, L7
- Vladilo G., Centurión M., Falomo R. & Molaro P., 1997, *A&A* 327, 47
- White R. L. & Becker R. H., 1992, *ApJS* 79, 331
- White R. L., Kinney A. L. & Becker R. H., 1993, *ApJ* 407, 456
- Wilkinson P. N., Browne I. W. A., Patnaik A. R., Wrobel J. M. & Sorathia B., 1998, *MNRAS* 300, 790
- Wolfe A. M. & Davis M. M., 1979, *AJ* 84, 699
- Wolfe A. M., Briggs F. H. & Jauncey D. L., 1981, *ApJ* 248, 460
- Wolfe A. M., Briggs F. H., Turnshek D. A. et al., 1985, *ApJ* 294, L67
- Wolfe A. M., Turnshek D. A., Smith H. E. & Cohen R. D., 1986, *ApJS* 61, 249.
- Wolfire M. G., Hollenbach D., McKee C. F., Tielens A. G. G. M. & Bakes E. L. O., 1995, *ApJ* 443, 152.
- Wright A. & Otrupcek R. (eds.), 1990, *Parkes catalogue*, Australia Telescope National Facility
- Young L. M. & Lo K. Y., 1997, *ApJ* 490, 710